Journal of Advanced Electrochemistry 2(1) (2016) 60–66

ISSN: 2455-0205

Contents List available at JACS Directory

Journal of Advanced Electrochemistry

journal homepage: http://www.jacsdirectory.com/jaec

Experimental and Computational Chemistry Studies on the Inhibition of the Corrosion of Mild Steel in 0.1 M H_2SO_4 by 4-Hydroxylbenzoic Acid

P.O. Ameh[1,*], P. Ukoha[2], P. Ejikeme[2], N.O. Eddy[3]

[1]*Department of Chemistry, Nigeria Police Academy, Wudil, Kano State, Nigeria.*
[2]*Department of Pure and Industrial Chemistry, University of Nigeria, Nsukka, Enugu State, Nigeria.*
[3]*Department of Chemistry, Federal University Lokoja, Kogi State, Nigeria.*

ARTICLE DETAILS

Article history:
Received 09 February 2016
Accepted 01 March 2016
Available online 17 March 2016

Keywords:
Corrosion
Mild Steel
Inhibition
4-Hydrobenzoic Acid

ABSTRACT

Weight loss, potentiodynamic polarization (PDP), linear resistant polarization (LPR) and electrochemical impedance spectroscopy (EIS) methods were used to investigate the inhibition potentials of various concentrations of 4-hydroxylbenzoic acid for mild steel corrosion in 0.1 M H_2SO_4. The surface morphology of the metal was studied using scanning electron microscope (SEM) while the Fourier transformed infra-red spectrophotometer was used to identified the functional groups participating in the inhibition process. Experimental results indicated that the inhibition efficiencies of 4-hydroxylbenzoic acid obtained from weight loss, PDP, LPR and EIS measurements at 303 K ranged from 56.21 to 69.35%, 81.03 to 91.03%, 68.17 to 94.64% and from 97.42 to 99.44% respectively. The inhibition efficiency exhibited a progressive increase with increase in concentration and a corresponding decrease with temperature. The SEM micrographs of the metals' surface, in the presence of the inhibitor revealed smoothness of the metal's surface through inhibition. Some functional groups of the inhibitor were missing; some were re-characterized by shifts in frequency of absorption while few new bonds were formed. The adsorption of 4-hydroxyl benzoic acid supported physical adsorption mechanism because the inhibition efficiency increases with temperature and the range of values obtained for the activation energy (41.40 to 66.22 J/mol) and the standard free energy of adsorption (-10.87 to -11.67 J/mol) were within the expected range for physiosorption. Calculated values of some electronic parameters were within the range of values expected for some known and efficient corrosion inhibitors while Results obtained from computational chemistry modeling are in strong agreement with experimental results.

1. Introduction

In recent times, industrial revolutions have led to increase in the used of some metals (such as mild steel, aluminum, zinc etc.) in the fabrication of some installations. Mild steel is an essential metal in most industries because it is ductile and malleable. It is strongly evident that metals are not free from corrosion as long as they have contact with aggressive medium, which can be acid, base, salt and some gases. Reported cases of severe corrosion attacks in some industries including fertilizer plant, oil exploration/refinery companies, metallurgical industries and other, have been evidently linked to some operational processes (such as acid wash, pickling, etc.) carried out using the metallic facilities [1, 2]. The use of corrosion inhibitors to retard the wearing away and subsequent destruction of metals in most industries, has been found to be one of the best preventive alternatives [3].

At minute concentration, corrosion inhibitors protects metal by reducing their corrosion rate. Several organic compounds are effective inhibitors for the corrosion of several metals in recent time and are characterized by suitable functional groups, aromatic system, π-electrons and long carbon chains [4-6]. Historical trends on the application of corrosion inhibitors have shown progresses from those inhibitors that contain heavy metal, costly and non-biodegradable to green corrosion inhibitors which are easily accessible, less expensive, biodegradable and ecofriendly [7].

Most green corrosion inhibitors are extracts of natural products but they suffer the set back of presenting less information on the actual chemical or functional structures that aid the adsorption of the inhibitor, which is the initial mechanism in corrosion inhibition. This limits the extent to which useful information and development can be reference for such inhibitors because corrosion inhibition efficiency is dependent on the chemical structure and some quantum parameters of the inhibitor [8, 9]. These challenges have prompted several researchers to screen the potentials of some compounds, as green inhibitors for the corrosion of some metals. These include some synthesized organic compounds, drugs, etc. The present study is aimed at investigating the corrosion inhibition potential of 4-hydroxylbenzoic acid for the corrosion of mild steel in solution of H_2SO_4 using gravimetric method (at 303, 313, 323 and 333 K), LPR, PDP and EIS at 303 K respectively. Computational chemistry calculations shall also be employed to correlate the inhibition efficiency of the compound with some electronic parameters and to predict locations for electrophilic and nucleophilic reactions.

4-hydroxylbenzoic acid is a phenolic derivative of benzoic acid and a white crystalline solid, which has a melting point of 487.60 K and acidity of 4.54 (k_a = 3.3 x 10^{-5} M at 292 K). 4-hydroxyl benzoic acid is found naturally in *Ganoderma lucidum* and in plants belonging to the *Vitex* genus, including *V. castus* and in *Hypericum perforatum*, *Spongiochloris spongiosa* (fresh water algae). It is highly biodegradable, an effective antioxidant and has a very low toxicity (LD_{50} = 2200 mg/kg in mice (oral dose)) [10]. The chemical structure of 4-hydroxylbenzoic acid is shown in Fig. 1. The compound has hydroxyl and carboxyl functional groups and possess aromatic ring in addition to other green properties. Energy minimization on the optimized structure of this compound shows that the two oxygen atoms in the hydroxyl groups (i.e., O-18 and O-19), each has lone pair of electron. Therefore, due to its unique properties, 4-hydroxylbenzoic acid is expected to be good green corrosion inhibitor. The authors of this article are unaware of reported cases involving the use of 4-hydroxyl benzoic acid as a corrosion inhibitor for mild steel in solution of H_2SO_4.

*Corresponding Author
Email Address: nocaseoche@yahoo.com (Paul O. Ameh)

Cite this Article as: P.O. Ameh, P. Ukoha, P. Ejikeme, N.O. Eddy, Experimental and computational chemistry studies on the inhibition of the corrosion of mild steel in 0.1 M H_2SO_4 by 4-hydroxylbenzoic acid, J. Adv. Electrochem. 2(1) (2016) 60–66.

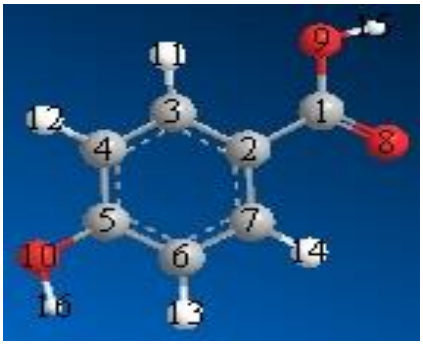

Fig. 1 3D structure of 4-hydroxyl benzoic acid

2. Experimental Methods

The inhibitor 4-hydroxylbenzoic acid was received from Aldrich store. The mild steel was purchased from a commercial market located within Abuja, Nigeria. The composition of the mild steel (in wt. %) as determined by quantiometric method is Mn (0.6%), P (0.36%), C (0.15%), Si (0.03%) and Fe (98.86%). Different coupons, each of dimensions, 4 x 5 x 0.05 cm were produced from the mild steel sheet and reserved for used in weight loss experiment. For the electrochemical experiments, the dimension of each coupon was 2 x 1.5 x 0.05 cm. Each coupon was polished with series of emery paper of variable grades, degrease by washing with ethanol, rinse in acetone and allowed to dry in the air and finally preserved in a desiccator.

2.1 Gravimetric Method

Gravimetric experiments were conducted at different temperatures (303, 313, 323 and 333 K) and with various concentrations of the inhibitor (0.002, 0.004, 0.006, 0.008 and 0.01 M) in 0.1 M H_2SO_4, which also served as the blank. Each experiment was conducted by inserting mild steel coupon (of known weight) into a 250 mL conical flask containing 150 mL of the test solution, whose temperature was kept constant using a water bath. The conical flask was covered with aluminum foil and kept for 168 hours. After every 24 hours, each coupon was withdraw, wash in distilled water containing 50% of zinc dust and allowed to dry in the air after rinsing with acetone. The difference in weight before and after immersion was recorded as weight loss.

The experiment was carried for different concentrations of the test solutions and for different temperatures, each for 168 hours, with allowance for weighing after every 24 hours.

From the gravimetric experiments, the corrosion rate, surface coverage (θ) and inhibition efficiency (%) were evaluated using the following equations [11]:

$$\%I = \frac{w_1 - w_2}{w_1} \times 100 \quad (1)$$

$$\theta = \left[1 - \frac{w_1}{w_2}\right] \quad (2)$$

$$CR = \frac{w_1 - w_2}{At} \quad (3)$$

where w_1 and w_2 are the weight losses of mild steel (in grams) in the absence and presence of the inhibitor respectively. θ is the degree of surface coverage of the inhibitor, CR is the corrosion rate of mild steel, A is the surface area of the mild steel coupon in cm^2 and t is the period of immersion in hours.

2.2 Electrochemical Impedance Spectroscopy (EIS)

The electrochemical experiment was carried out using two concentrations (0.001 and 0.015 M) of the test solution and with a VERSASTAT 400 complete DC voltammetry and corrosion system, having, V3 studio software. A test coupon with 1 cm^2 exposed areas was used as working electrode and a graphite rod as counter electrode. The reference electrode was the saturated calomel electrode. All experiments were undertaken in stagnant aerated solutions at 30±1 °C. The working electrode was immersed in a test solution for one hour until a stable open circuit potential was attain. From the electrochemical measurements, the real part was plotted on the X-axis and the imaginary part, on the Y-axis of a chart to develop a Nyquist Plot. The charge transfer resistance values (R_{ct}) were calculated from the difference in impedance at lower and higher frequencies [12]. The frequency at which the imaginary component of the impedance at maximum f (−Z″img) was found and the double-layer capacitance (C_{dl}) values was calculated using Eq. (4) [13].

$$f\left(-Z''_{img}\right) = \frac{1}{2\pi} C_{dl} R_{ct} \quad (4)$$

The inhibition efficiency of 4-hydroxyl benzoic acid was calculated from the charge transfer resistance values using Eq. (5) [14].

$$\%I = \frac{R_{ct(Inh)} - R_{ct}}{R_{ct(Inh)}} \times \frac{100}{1} \quad (5)$$

where, R_{ct} and $R_{ct(inh)}$ are the charge transfer resistance values in the absence and presence of inhibitor for mild steel in 0.1 M H_2SO_4, respectively.

2.3 Potentiodynamic Polarisation

The potentiodynamic current-potential curves were recorded by changing the electrode potential, E_{corr} automatically with a scan rate 0.33 mVs^{-1} from a low potential of -800 to -300 mV (SCE). Before each run, the working electrode was immersed in the test solution for 30 minute until a steady state was achieved. The linear Tafel segments of the anodic and cathodic curves obtained were extrapolated to corrosion potential to obtain the corrosion current densities (i_{corr}) and the inhibition efficiency (I%) was evaluated from the measured i_{corr} values using Eq. (5) [15].

$$\%I = \frac{i^0_{Corr} - i_{Corr}}{i^0_{Corr}} \times \frac{100}{1} \quad (6)$$

where i^0_{Corr} and i_{Corr} are the uninhibited and inhibited corrosion current densities, respectively.

2.4 Linear Polarization Resistance

Linear polarization resistance measurements were carried out within the potential range of ± 20 mV with respect to the open circuit potential. The corresponding current was recorded at a scan rate of 0.5 mV/S. From the results obtained, values of the over potential was plotted against current and from the slope of the plot, the polarization resistant (R_p) was obtained. From the measured R_p values, the inhibition efficiency (I %) was calculated using Eq. (7):

$$\%I = \frac{R_{p(Inh)} - R_p}{R_{p(Inh)}} \times \frac{100}{1} \quad (7)$$

where R_p and $R_{p(inh)}$ are the uninhibited and inhibited polarization resistance, respectively.

2.5 Scanning Electron Microscopy

A scanning electron microscope (SEM) model JSM-5600 LV, was used to take the micrograph of mild steel surface withdraw from solution of H_2SO_4, in the absence and in the presence of 0.008 M of the inhibitor. The sample was mounted on a metal stub, make conductive by sputtering with gold and the image was taken at different magnifications using accelerating voltage of 10 kV.

2.6 FTIR Analysis

FTIR spectra of the corrosion products of mild steel (withdraw from test solution of 0.1 M H_2SO_4) in the absence and presence of 0.008 M 4-hydroxylbenzoic acid were taken using Shimadzu FTIR-8400S Fourier transform infra-red spectrophotometer. The sample was sensitize with KBr and the scanning was done within a wave number range of 400 to 4000 cm^{-1}.

2.7 Quantum Chemical Calculations

Chemical structure of 4-hydroxyl benzoic acid was drawn using ChemBio software and the structure was saved as hyperchem ISSI input file. This was followed by successful geometric optimization using PM6, Ab initio and DFT programmes in the software. Muliken charges of the cationic, neutral and anionic forms of the inhibitor were calculated using the Hyperchem software while semi empirical parameters were calculated using MOPAC software.

3. Results and Discussions

3.1 Gravimetric Study

Results obtained for weight loss of mild steel in 0.1 M H_2SO_4 after every 24 hours were used to develop plots of weight loss versus time at various temperatures as shown in Figs. 2a-d. The plots reveal that weight loss of mild steel generally increases as the period of contact increases but decreases with increasing concentration of the inhibitor. Consequently, since weight loss is proportional to the rate of corrosion, it can be inferred that the rate of corrosion of mild steel in solution of H_2SO_4 increases with increase in the period of contact but decreases with increase in the

concentration of 4-hydroxyl benzoic acid. This also implies that 4-hydroxyl benzoic acid inhibited the corrosion of mild steel in solution of H_2SO_4 by retarding its corrosion rate. Weight loss of mild steel (hence corrosion rate of mild steel) was also found to increase with increase in temperature.

In Table 1, values of corrosion rate of mild steel in solutions of H_2SO_4, and inhibition efficiencies of various concentrations of 4-hydroxylbenzoic acid are recorded. The results obtained reveal that the inhibition efficiency of various concentrations of 4-hydroxylbenzoic acid increases with increase in concentration but decreased with increasing temperature. The observed trend is consistent with finding obtained for most adsorption inhibitors that follow the mechanism of physical adsorption [16, 17]. Generally, what characterize an adsorption inhibitor is an increase in inhibition efficiency with increasing concentration and if the extent of adsorption (as measured by inhibition efficiency) decreases with increase in temperature, the mechanism of physical adsorption is favoured as manifested in the present study [17].

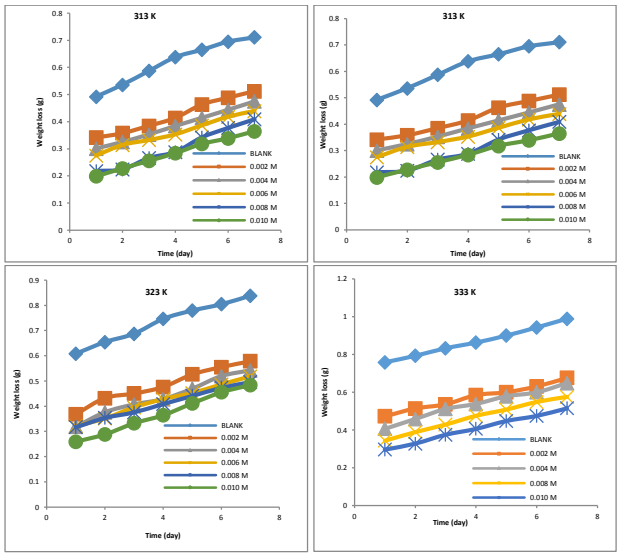

Fig. 2 Variation of weight loss with time for the corrosion of mild steel in 0.1 M H_2SO_4 containing various concentrations of 4-hydroxyl benzoic acid at 303, 313, 323 and 333 K

Table 1 Corrosion rate of mild steel in solution of 0.1 M H_2SO_4 and inhibition efficiencies of 4- hydroxylbenzoic acid for mild steel in 0.1 M H_2SO_4

C (M)	Corrosion rate ($gh^{-1}cm^{-2}$)				Inhibition efficiency (%)			
	303 K	313 K	323 K	333 K	303 K	313 K	323 K	333 K
Blank	0.00366	0.00522	0.09440	0.01686	-	-	-	-
0.002	0.00145	0.00229	0.00636	0.01243	60.12	56.21	38.84	26.25
0.004	0.00129	0.00217	0.00604	0.01122	67.26	59.95	40.94	33.43
0.006	0.00122	0.00186	0.00586	0.01083	69.25	64.24	41.73	35.52
0.008	0.00099	0.00175	0.00573	0.01062	73.61	66.65	42.05	36.90
0.010	0.00090	0.00151	0.00556	0.01010	75.53	69.35	46.65	40.44

3.2 Potentiodynamic Polarization Measurements

Fig. 3 shows potentiodynamic plots for the corrosion of mild steel in 0.1 M H_2SO_4 containing 0.001, 0.010 and 0.015 M of 4-hydroxyl benzoic acid in 0.1 M H_2SO_4 at 303 K. Polarizarion data including Tafel constants, corrosion current, corrosion potential and calculated inhibition efficiencies are presented in Table 2. Also presented in Table 2 are values of polarization resistant and the corresponding inhibition efficiency obtained from LPR method. The results obtained from the PDP measurements clearly reveal that I_{corr} becomes more negative (i.e. decreases) as the concentration of the inhibitor increases. This implies that 4-hydroxylbenzoic acid retarded the corrosion of mild steel in solution of H_2SO_4. It was also notice from the data that the displacement of the corrosion potentials (due to the presence of various concentrations of 4-hydroxyl benzoic acid) from the measured potential of the blank was less than 85 mV. Therefore, 4-hydroxyl benzoic acid is a mixed type inhibitor for the corrosion of mild steel in solution of H_2SO_4. This findings was also supported by the seemingly similarity in the displacement of the anodic and cathodic arms of the Tafel plots (Fig. 3) and the relative small difference between the cathodic and anodic Tafel constants. Generally, mixed type inhibitors protect metals against corrosion in three major ways, namely, by mechanism of physical adsorption, by mechanism of chemical adsorption and by the formation of a protective film. In this study, it has been confirmed that physical adsorption is the prevailing adsorption mechanism. However, owing to the excellent inhibition efficiencies obtained for various concentrations of 4-hydroxyl benzoic acid, it is significant to state that 4-hydroxyl benzoic acid protected mild steel against corrosion by the forming a protective film [18].

LPR data reveals that the polarization resistant data increase as the concentration of the inhibitor increases. Therefore, the inhibition efficiency of the inhibitor also increases with increase in concentration. Values of inhibition efficiency obtained from PDP and LPR correlated excellently.

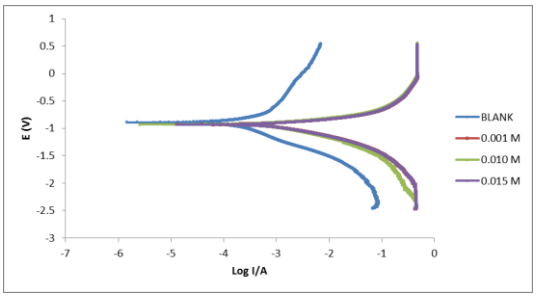

Fig. 3 Potentiodynamic polarization curves for the mild steel steel in 0.1 M H_2SO_4 in the absence and presence of different concentrations of 4-hydroxybenzoic acid

Table 2 Polarization data for the corrosion of mild steel in 0.1 M H_2SO_4 in the absence and presence of 4-hydroxyl benzoic acid at 303 K

C (M)	LPR		PDP				
	R_p (Ω/cm^2)	%I	β_a $mVdec^{-1}$	β_c $mVdec^{-1}$	E_{corr} (mV)	I_{corr} (μA)	I %
Blank	20.40	-	139.4	146.1	- 863	210. 36	-
0.001	64.22	68.17	111.7	131.2	-906	39.75	81.03
0.010	124.62	83.63	110.0	128.5	- 927	25.75	87.59
0.015	380.89	94.64	107.3	125.3	-933	12.88	91.03

Table 3 EIS parameters for corrosion of mild steel in 0.1 M H_2SO_4 in the absence and presence of different concentrations of 4-hydroxyl benzoic acid at 303 K

C (M)	R_{ct}, Ω cm^2	R_s, Ω cm^2	C_{dl}, μF cm^{-2}	%I
Blank	27.8920	4.522	2320	-
0.001	1495.760	99.001	1753	97.42
0.015	4575.811	105.590	1250	99.44

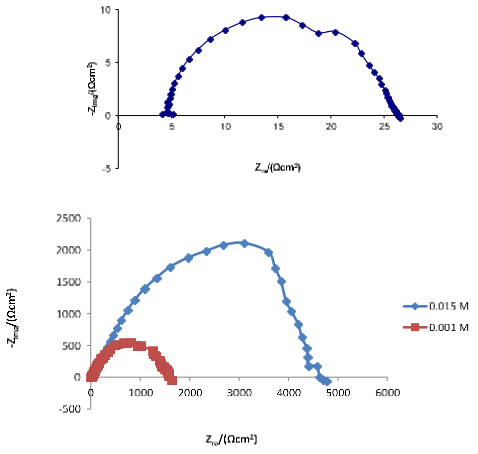

Fig. 4 Nyquist plots for the mild steel in 0. 1 M H_2SO_4 in the absence and presence of different concentrations of 4-hydroxybenzoic acid

3.3 Electrochemical Impedance Spectroscopy (EIS)

EIS data obtained from experiment are recorded in Table 3 while the Nyquist plot developed from the data (for blank and inhibited systems) are presented in Fig. 4. The figure reveals that the curves are single capacitive semicircles and that the diameter of the semi–circles increases as the concentration of 4-hydroxyl benzoic acid increases. Therefore, the corrosion process is control by charge transfer even as 4-hydroxyl benzoic acid retarded the corrosion reaction [19]. The shapes of the curves were relatively parallel to each other, which suggests similarity in corrosion mechanism [20]. The charge transfer resistant was found to increase with

increase in the concentration of the inhibitor while the solution resistant and the double layer capacitance decrease with increasing concentration. Increase in the magnitude of charge transfer resistant is associated with retardation of corrosion (i,e inhibition) while decrease in C_{dl} points toward decreasing dielectric constant and hence better inhibition efficiency.

3.4 Effect of Temperature

The relationship between temperature and the rate of reaction can be investigated using the Arrhenius equation, which equates the rate of a chemical reaction to be proportional to the exponent of the activation energy divided by RT as expressed in Eq. (8) [21].

$$CR = Aexp\left(\frac{-E_a}{RT}\right) \quad (8)$$

where CR is the corrosion rate of mild steel, A is the Arrhenius or pre-exponential factor, E_a is the activation energy, R is the universal gas constant and T is the temperature. Eq. (7) can be linearized by taking the logarithm of both sides of the equation and the result is expressed as Eq. (9).

$$\ln(CR) = \ln(A) - \frac{E_a}{RT} \quad (9)$$

Eq. (9) is a linear model that translates to a straight line if values of ln(CR) is plotted against 1/T and would be characterized by slope and intercept equal to E_a/R and ln(A) respectively. Fig. 5 shows the Arrhenius plots for the corrosion of mild steel in H_2SO_4, in the absence and presence of various concentrations of 4-hydroxyl benzoic acid. Calculated values of the activation energy, the Arrhenius constant and degree of linearity are recorded in Table 4. The results obtained support the application of the Arrhenius model to the present data through excellent degree of fitness (values of R^2 were very close to unity). The activation energies obtained from the slopes of plots in Fig. 5 ranged from 62.08 to 71.14 J/mol while the activation energy for the blank was 43.25 J/mol. From the obtained range and the significant difference between the activation energy of the uninhibited and those of the inhibited systems, the adsorption of 4-hydroxyl benzoic acid on mild steel surface is consistent with the mechanism of charge transfer from charged inhibitor to charged metal surface [22].

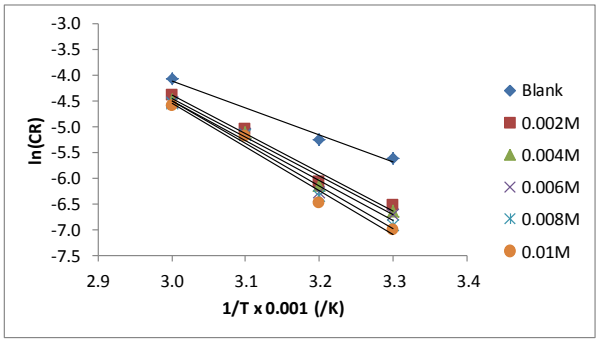

Fig. 5 Arrhenius plot for the corrosion of mild steel in 0.1 M H_2SO_4 containing various concentrations of 4-hydroxyl benzoic acid

Table 4 Arrhenius and transition state adsorption parameters for the corrosion of mild steel in 0.1 M H_2SO_4 containing various concentration of 4-hydroxylbenzoic acid

C(M)	Arrhenius parameters			Transition state parameters				
	Ln(A)	E_a (J/mol)	R^2	slope	intercept	ΔS^0_{ads} (J/mol)	ΔH^0_{ads} (J/mol)	R^2
Blank	11.489	43.25	0.9881	-4.8877	4.7389	-40.64	-45.24	0.9863
0.002	18.006	62.08	0.9812	-7.1524	11.254	-59.47	8.93	0.9795
0.004	18.059	62.46	0.9848	-7.1982	11.316	-59.85	9.44	0.9834
0.006	18.583	64.00	0.971	-7.3833	11.831	-61.38	13.73	0.9685
0.008	20.416	69.04	0.9799	-7.9898	13.663	-66.43	28.96	0.9783
0.010	21.131	71.14	0.9701	-8.2425	14.378	-68.53	34.90	0.9678

3.5 Adsorption/Thermodynamic Considerations

The equation that relates thermodynamic parameters with the rate of corrosion and temperature is the Transition state equation, which can be written according to Eq. (10) [23].

$$CR = \frac{RT}{Nh} exp\left(\frac{\Delta S^0_{ads}}{R}\right) exp\left(\frac{-\Delta H^0_{ads}}{RT}\right) \quad (10)$$

where CR is the corrosion rate, T is the temperature, N is the Avogadro's number, his the Plank constant, ΔS^0_{ads} is the standard entropy change of adsorption and ΔH^0_{ads} is the standard enthalpy change of adsorption. Conversion of Eq. (10) to a linear model yields Eq. (11),

$$ln\left(\frac{CR}{T}\right) = ln\left(\frac{R}{Nh}\right) + \frac{\Delta S^0_{ads}}{R} - \frac{\Delta H^0_{ads}}{RT} \quad (11)$$

Fig. 6 shows the Transition state plots of values obtained for $ln\left(\frac{CR}{T}\right)$ versus 1/T for the corrosion of mild steel in solutions of H_2SO_4 containing various concentrations of 4-hydroxyl benzoic acid. Data obtained from the plots are presented in Table 4. The results reveal that R^2 ranged from 0.9678 to 0.9863 indicating excellent degree of linearity. ΔH^0_{ads} for the blank was -40.64 J/mol while ΔH^0_{ads} values in the presence of various concentrations of the inhibitor have average value of -63.13 J/mol indicating that the adsorption of the inhibitor on the surface of mild steel is exothermic and occurs with increasing heat of adsorption as the concentration of the inhibitor increases. ΔS^0_{ads} values (in the presence of the inhibitor) were found to fall within the range, 8.93 to 34.90 J/mol while ΔS^0_{ads} value for the blank was -40.64 J/mol. Normally, positive value of ΔS^0_{ads} reflects non feasibility of the adsorption process but ΔS^0_{ads} is not a unique parameter for predicting the direction of a reaction. From thermodynamics, a spontaneous reaction is characterized by negative value of ΔG^0_{ads}. When ΔS^0_{ads} is positive, ΔG^0_{ads} can be negative provided ΔH^0_{ads} is negative or $\Delta H^0_{ads} < T\Delta S^0_{ads}$. Therefore, the adsorption of 4-hydroxyl benzoic acid on the surface of mild steel is exothermic and spontaneous.

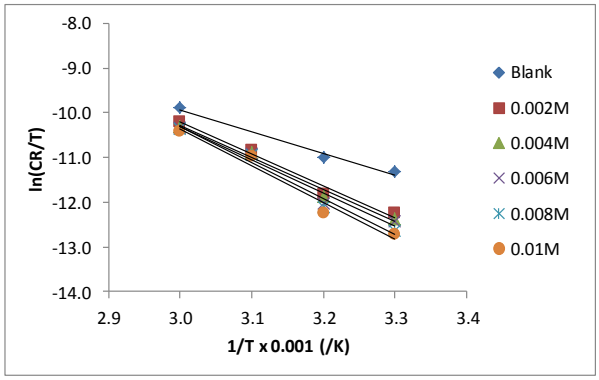

Fig. 6 Transition state plot for the corrosion of mild steel in 0.1 M H_2SO_4 containing various concentrations of 4-hydroxylbenzoic acid

It has been established that the mechanism of inhibition of mild steel corrosion in solution of H_2SO_4 by 4-hydroxyl benzoic acid is physical adsorption. The adsorption characteristics of this inhibitor can be further analyzed using adsorption isotherms. Data were fitted to different isotherms to obtain the best fitted isotherms and it was found that the Langmuir and Frumkin adsorption models best described the adsorption characteristics of 4-hydroxyl benzoic acid unto mild steel surface. The expression of the Langmuir adsorption model is according to Eq. (12) [24].

$$ln\left(\frac{C}{\theta}\right) = lnC + ln\left(\frac{1}{b_{ads}}\right) \quad (12)$$

Eq. (12) is a linear model, which indicates that a plot of $ln\left(\frac{C}{\theta}\right)$ versus ln(C) should be a straight line with slope and intercept equal to unity and $ln\left(\frac{1}{b_{ads}}\right)$ respectively. The Langmuir isotherm for the adsorption of 4-hydroxyl benzoic acid on mild steel surface is presented in Fig. 7. Adsorption data obtained from the slopes and intercepts of the plots are recorded in Table 5. Proximity of the calculated R^2 values to unity indicates the suitability of the Langmuir adsorption model to the present data. However, slope values, which ranged from 0.748 to 0.9073 show slight deviation from the ideal value of unity. Therefore, there is slight interaction between the adsorbed species. According to Eddy *et al* [11], the Frumkin adsorption model accounts for the existent of interaction in the Langmuir model and that the Frumkin model becomes the Langmuir model when there is no interaction. In the light of this, the Frumkin model Eq. (13) was also found to fit our data excellently.

$$\frac{\theta}{1-\theta} e^{-2a\theta} = b_{ads}C \quad (13)$$

Cite this Article as: P.O. Ameh, P. Ukoha, P. Ejikeme, N.O. Eddy, Experimental and computational chemistry studies on the inhibition of the corrosion of mild steel in 0.1 M H_2SO_4 by 4-hydroxylbenzoic acid, J. Adv. Electrochem. 2(1) (2016) 60–66.

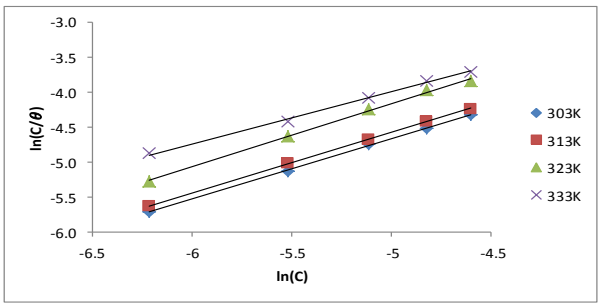

Fig. 7 Langmuir isotherm for the adsorption of 4-hydrobenzoic acid on mild steel surface

Table 5 Langmuir and Frumkin parameters for the adsorption of 3-nitrobenzoic acid on the surface of mild steel

Isotherm	T (K)	Slope	$\log b_{ads}$	'a'	$\Delta G^0_{ads}(\frac{kJ}{mol})$	R^2
Langmuir	303	0.7982	0.3396	-	-12.09	0.9982
	313	0.8097	0.2648	-	-11.65	0.9927
	323	0.7939	0.2654	-	-11.66	0.9999
	333	0.7611	0.2763	-	-11.72	0.9988
Frumkin	303	1.4369	3.116	1.56	-17.97	0.9982
	313	1.3505	2.392	1.20	-16.14	0.998
	323	1.1606	0.5226	0.26	-11.43	0.994
	333	1.2742	1.3101	0.66	-13.42	0.9978

All parameters are as defined before. A linear model of Eq. (13) can be best derived by taking the logarithm of both sides of the equation as expressed in Eq. (14),

$$ln\left(\frac{\theta}{1-\theta}\right) * \left[\frac{1}{C}\right] = lnb_{ads} + 2a\theta \qquad (14)$$

The Frumkin isotherms for the adsorption of 4-hydroxyl benzoic acid are presented in Fig. 8 while adsorption parameters deduced from the plots are also presented in Table 5. R^2 values for the plots, which ranged from 0.994 to 0.9982, were significant in defining an excellent degree of fitness of the adsorption data to the Frumkin model. The interaction parameters are found to be positive (i.e. 1.86, 1.20, 0.26 and 0.66 at 303, 313, 323 and 333 K respectively), which point toward the attractive behavior of the inhibitor.

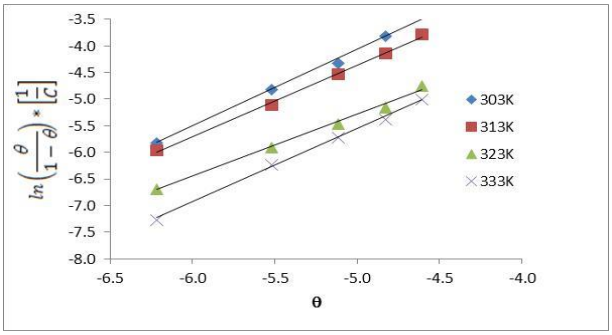

Fig. 8 Frumkin isotherm for the adsorption of 4-hydrobenzoic acid on mild steel surface

Thermodynamic feasibility of a given process such as adsorption can be assess using the value of the standard free energy change, ΔG^0_{ads}, which is related to the equilibrium constant of adsorption (b_{ads}) according to Eq. (15) [25, 26],

$$b_{ads} = -\frac{1}{55.5} exp\left(\frac{\Delta G^0_{ads}}{RT}\right) \qquad (15)$$

Values of ΔG^0_{ads} obtained from b_{ads} and through the Langmuir and Frumkin isotherms are presented in Table 5. These values ranged from -9.76 to -11.81 kJ/mol (average = -10.91 kJ/mol) and from -14.75 to -17.97 kJ/mol (average = -15.34 kJ/mol) for the Langmuir and Frumkin functions respectively. Therefore, the adsorption of 4-hydroxyl benzoic acid is spontaneous and favours physical adsorption mechanism.

3.6 SEM Study

Fig. 9 shows the SEM micrographs (taken at 1000 x 1500 x and 5000 x magnifications) of the surface of mild steel withdrawn from (a) 0.1 M H_2SO_4 (b) 0.1 M H_2SO_4 containing 0.006 M of the inhibitor. Examination of the two set of micrographs reveals that the surfaces of the metal coupons from solution of H_2SO_4 are very rough but in the presence of 4-hydroxyl benzoic acid, the surfaces are smooth. These confirm that 4-hydroxyl benzoic acid form a protective film on the surface of the metal and thus inhibit its corrosion.

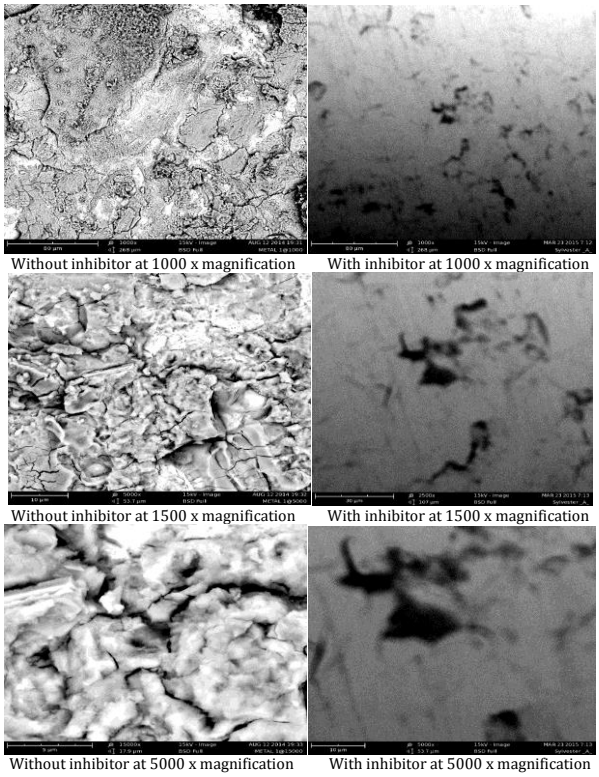

Fig. 9 Scanning electron micrographs of the corrosion product of mild steel in the absence and presence of 4-hydroxyl benzoic acid (as an inhibitor) at various magnifications

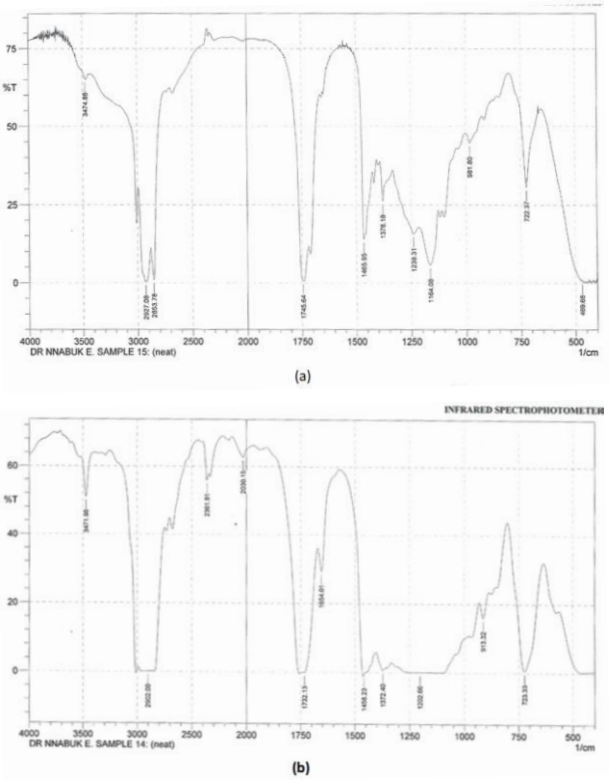

Fig. 10 FTIR spectrum of (a) 4-hydroxyl benzoic acid (b) corrosion product of mild steel in the presence of 4-hydroxyl benzoic acid as an inhibitor

3.7 FTIR Study

The major application of FTIR in corrosion study is to identify the functional group associated with the absorption of the inhibitor on the surface of the metal. FTIR spectrum of 4-hydroxyl benzoic acid is shown in

Fig. 10 presents the FTIR spectrum of the corrosion product of mild steel, inhibited by 4-hydroxyl benzoic acid. Peaks and wave number of IR adsorption deduced from the spectra are presented in Table 6. The major remarks that can be deduced from the presented results can be grouped into three including,

(i) A shift in functional groups as a result of interaction between 4-hydroxyl benzoic acid and the metal surface. The affected functional groups included carbon ring vibration, C-O stretch, CH_3 deformation, C=O stretch, C-H stretch and OH stretch. In all these cases, the shifts resulted in reducing the intensity of the functional group.

(ii) Missing functional groups were C-O stretch at 1164 cm^{-1} and C-H stretch at 2853 cm^{-1}. These functional groups might have been used in forming new bonds.

(iii) Functional groups associated with the formation of new bonds were C=O stretch at 1654 cm^{-1} and C=C stretch at 2382 cm^{-1}.

From the above analysis, we can state that there is interaction, formation of new bonds and adsorption of the inhibitor unto the mild steel surface.

Table 6 Frequencies and peak of IR absorption by 4-hydroxyl benzoic acid and the corrosion product of mild steel in the presence of 4-hydroxyl benzoic acid

4 hydroxyl benzoic acid			Inhibited corrosion product		
Frequency (cm^{-1})	intensity	Functional group	Frequency (cm^{-1})	Intensity	Functional group
469.68	0.619				
722.37	30.649		723.33	0.612	
961.80	44.661	Carbon ring vibration	913.32	15.959	Carbon ring vibration
1164.08	5.805	C-O stretch			
1239.31	15.641	C-O stretch	1202.66	0.118	C-O stretch
1378.18	26.269	CH_3 deformation	1372.40	0.699	CH_3 deformation
1465.95	13.939	Aromatic C=C stretch	1458.23	0	
			1654.01	29.372	C=O stretch
1745.64	0.593	C=O stretch	1732.13	0	C=O stretch
			2030.15	62.637	
			2381.91	55.911	C=C stretch
2853.78	0.957	C-H stretch			
2927.06	0.321	C-H stretch	2902.00	0.139	C-H stretch
3474.88	65.270	OH stretch	3471.98	50.971	OH stretch

3.8 Computational Chemistry Study

3.8.1 Global Reactivity

Global reactivity embraces indices that are associated with the reactivity of the entire molecule and not on the atoms that make up the molecule. In this study, global reactivity was considered in terms of semi empirical parameters including the energy of the highest occupied molecular orbital (E_{HOMO}), the energy of the lowest unoccupied molecular orbital (E_{LUMO}), the binding energy (E_b), the electronic energy (E_{Elect}), the core core repulsion energy (E_{CCR}), the dipole moment (μ), the heat of formation (H_f) and the total energy of the molecule (E_T). The frontier molecular orbital energies (E_{HOMO}, E_{LUMO} and the energy gap, $E_{L\text{-}H}$) are very essential in determining the reactivity of a molecular species. It is generally agreed that increase in $E_{HOMO}$and decrease in the values of E_{LUMO} and $E_{L\text{-}H}$ are associated with better inhibition efficiency.

Table 7 Calculated Semi empirical parameters of 4-hydroxylbenzoic acid for various Hamiltonians

Models	E_{HOMO} (ev)	E_{LUMO} (eV)	E_b (eV)	E_{Elect} (eV)	E_{CCR} (eV)	μ (Debye)	H_f (eV)	E_{TE}
PM3	-9.59	-0.50	-1799	-179980	138398	1.96	-112.16	-41581
AMI	-9.48	-0.434	-1789	-184740	140003	1.86	-101.82	-44737
RMI	-9.37	-0.41	-1188	-184025	139888	1.78	498.54	-44137
MNDO	-9.37	-0.53	-1792	-185140	140257	1.75	-104.73	-44882
CNDO	-12.08	2.21	-5157	-225834	157150	1.30	-3470.12	-68683

Calculated values of the frontier molecular energies as presented in Table 7 for various Hamiltonians are in good agreement with those obtained for effective corrosion inhibitors [27-31]. The E_b, the E_{Elect}, the E_{CCR}, the E_T and the H_f are all essential parameters that have been proven to be associated with corrosion inhibition ability of a compound. Generally, the lower the lower the values of these energies, the better is the inhibition efficiency is expected. These parameters also within the range of values expected for some efficient corrosion inhibitors.

3.8.2 Local Selectivity

Local selectivity approach to reaction considers the reactivity of a molecule as a function of an atom or chemical bond and not the entire molecule. Hence active centers of a molecule are assumed to be resident in atoms or bonds within the molecule. Corrosion inhibition involves charge transfer from inhibitor to charged metal surface (physiosorption mechanism) or electron transfer from inhibitor to vacant d-orbital of the metal. Indeed corrosion inhibition involves electrophilic and nucleophilic substitution. The Fukui function (f) is widely used in considering the local reactivity of a molecular species. The Fukui function (f) can be formally defined as [11],

$$f(r) = \left(\frac{\delta\rho(r)}{\delta N}\right)_v \quad (16)$$

where ρ is the density of electron, N is the number of electron and v is the external potential. In considering an N electron system, when nucleophilic and electrophilic substation is involves, the N system will either change to N-1 system and N+1 system. This is consistent with the finite method approximation, which states that owing to discontinuity of the Fukui function, its value will differ when approaching from left or right. Hence we defined nucleophilic and electrophilic Fukui functions as follows [32],

$$f^+(r) = \left(\frac{\delta\rho(r)}{\delta N}\right)_v^+ = \left(\frac{\delta\mu}{\delta v(r)}\right)_N^+ = \rho_{N+1}(\mathrm{r}) - \rho_N(\mathrm{r}) \quad (17)$$

$$f^-(r) = \left(\frac{\delta\rho(r)}{\delta N}\right)_v^- = \left(\frac{\delta\mu}{\delta v(r)}\right)_N^- = \rho_N(\mathrm{r}) - \rho_{N-1}(\mathrm{r}) \quad (18)$$

Eq. (17) is applicable when N increase from N to N+1 while Eq. (18) applies to N decreasing from N to N-1. Therefore, the molecular sites with large value of f^+ are the sites where the molecule will receive charge when attacked by a nucleophile while the sites with large value of f^- are the sites through which the molecule will donate charge when attack by an electrophile. However, in practice, the condensed Fukui function is more useful. This is achieved by considering Muliken or Hirshfiled charges on each atom, instead of electron density. This we have,

$$f_x^+(r) = q_{N+1}(\mathrm{r}) - q_N(\mathrm{r}) \quad (19)$$

$$f_x^-(r) = q_N(\mathrm{r}) - q_{N-1}(\mathrm{r}) \quad (20)$$

Calculated values of $f_x^+(r)$ and $f_x^-(r)$ for 4-hydroxyl benzoic acid are presented in Table 8 for Ab initio and DFT levels of theory. From the data presented, Ab initio level of theory predicts the sites, C(1) and O(8) as those having highest value of $f_x^-(r)$ while DFT presents O(8). Therefore charge is transfer from 4-hydroxyl benzoic acid via O(8) atom to the metal surface and the adsorption is facilitated through this site. On the other hand, Ab initio results indicated that values of $f_x^+(r)$ are all negative, which is not physically significant while electrophilic attack is positioned on O(8) and O(9) atoms, under DFT model. Similar findings are presented in the HOMO and LUMO molecular orbitals in Fig. 11 (red represent positive while blue represent negative). It is significant to state that the HOMO correspond to $f_x^-(r)$ while the LUMO correspond to $f_x^+(r)$.

Table 8 Fukui function for electrophilic and nucleophilic attacks on carbon and electronegative atoms in the studied inhibitorcalculated from Muliken(Lowdin) charges using Abinitio

Atom No.	Extended Huckel charges	Ab initio		DFT	
		f^+	f^-	f^+	f^-
1 C	0.553017	-0.031637	0.132417	-0.092005	0.064719
2 C	-0.046568	-0.154608	0.083383	-0.082153	0.148950
3 C	0.011198	-0.054634	0.059374	-0.051061	0.041731
4 C	-0.100359	-0.033068	0.013506	-0.091386	-0.099328
5 C	0.275405	-0.030713	0.084174	-0.053573	0.200358
6 C	-0.102086	-0.052535	0.010787	-0.118917	-0.035556
7 C	0.011011	-0.029175	0.057761	-0.057587	-0.067759
8 O	-0.703345	-0.188018	0.125433	0.209881	0.210770
9 O	-0.150254	-0.052375	0.043358	0.127273	0.040772
10 O	-0.212828	-0.039630	0.036509	-0.527606	0.146785

In spite of identification of the O(8) atom as the site for the adsorption of 4-lhydroxy benzoic acid unto mild steel surface, it is obvious that the contribution of the entire carboxylic bond cannot be over ruled. The bond length for C(1)-O(9), C(5)-O(10) and C(1)-O(8) are 1.349, 1.359 and 1.225 Å. Generally, the higher the bond length, the more reactive the molecule is expected indicating that C(5)-O(10) bond supposed to be the most reactive bond. Secondly, energy minimization of the 4-hydroxyl benzoic acid reveals that O(10) and O(9) atoms, each has a lone pair of electron.

Cite this Article as: P.O. Ameh, P. Ukoha, P. Ejikeme, N.O. Eddy, Experimental and computational chemistry studies on the inhibition of the corrosion of mild steel in 0.1 M H_2SO_4 by 4-hydroxylbenzoic acid, J. Adv. Electrochem. 2(1) (2016) 60–66.

However, extended Huckel charges calculations (Table 8) reveals that the most positive charged atom in the inhibitor is on the C(1) atom. It is significant to state that the carboxylic functional group in the aromatic ring is more reactive than the hydroxyl group, explaining why the adsorption of 4-hydroxyl benzoic acid is preferably achieved through the carboxyl functional group.

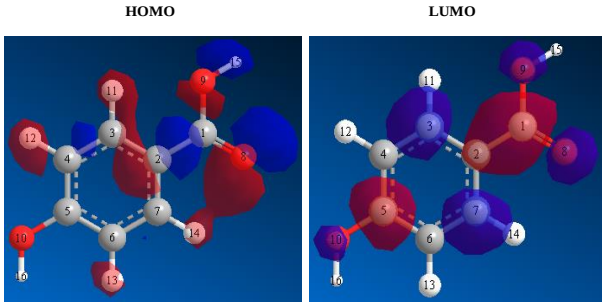

Fig. 11 HOMO and LUMO diagrams of 4-hydroxybenzoic acidcalculated from extended Huckel theory. The HOMO and LUMO diagram obtained at a potential of -12.00 eV and -2.759 eV respectively.

4. Conclusion

The results and findings of this study reveal that 4-hydroxyl benzoic acid is an efficient corrosion inhibitor for mild steel in solution of H_2SO_4. Average inhibition efficiency (obtained from weight loss measurements) is slightly lower than instantaneous inhibition efficiency (obtained from LPR, PDP and EIS). SEM micrographs of the metal surface after corrosion greatly indicated that the inhibitor is a mixed type inhibitor and forms a protective film over the metal surface. Computational chemistry modeling provides strong background for modeling the corrosion inhibition behavior of the studied inhibitor and the results obtained are in strong agreement with experimental results.

References

[1] P. Ameh, N. Eddy, *Commiphora pedunculata* gum as a green inhibitor for the corrosion of aluminium alloy in 0.1 M HCl, Res. Chem. Intermed. 40 (2014) 2641-2649.
[2] R.A.M. Anaee, Sodium silicate and phosphate as corrosion inhibitors for mild steel in simulated cooling water system, Arab. J. Sci. Eng. 39 (2014) 153-162.
[3] J. Zhang, J. Wang, F. Zhu, M. Du, Investigation of inhibition properties of Sophoro lipids for X65 steel corrosion in simulated oilfield produced water saturated with carbon dioxide, Ind. Eng. Chem. Res. 54 (2015) 5197-5203.
[4] A.C. Bastos, M.G. Ferreira, A.M. Simoes, Corrosion inhibition by chromate and phosphate extracts for iron substrates studied by EIS and SVET, Corr. Sci. 48 (2006) 1500-1512.
[5] E. Samiento-Bustos, J.G. Gonzalez Rodriguez, J. Uruchurtu, J. Dominguez-Patino, V.M. Salinas-Bravo, Effect of inorganic inhibitors on the corrosion behavior of 1018 carbon steel in the LiBr + ethylene glycol + H_2O mixture, Corr. Sci. 50 (2008) 2296-2303.
[6] G. Mu, X. Li, Q. Qu, J. Zhou, Molybdate and tungstate as corrosion inhibitors for cold rolling steel in hydrochloric acid solution, Corr. Sci. 48 (2006) 445-459.
[7] M. Yadav, R.R. Sinha, S. Kumar, T.K. Sarkar, Corrosion inhibition effect of spiropyrimidinethiones on mild steel in 15 % HCl solution: insight from electrochemical and quantum studies, RSC Adv. 5 (2015) 70832-70848.
[8] F.C. Giacomelli, C. Giaomelli, M.F Amadori, V. Schmidt, A. Spinelli, Inhibitor effect of succinic acid on the corrosion resistance of mild steel electrochemical, gravimetric and optical microscopic studies, Mater. Chem. Phy. 83 (2004) 124-128.
[9] M. Sahin, G. Gece, F. Karci, S. Bilgic, Experimental and theoretical study of the effect of some heterocyclic compounds on the corrosion of low carbon steel in 3.5% NaCl medium, J. Appl. Electrochem. 38 (2006) 809-815.
[10] R.J. Lewis, Dangerous properties of industrial materials, 9th Ed., Van Nostrand Reinhold, New York, 1996, pp.1-3.
[11] N.O. Eddy, U.J. Ibok, P.O. Ameh, N.O. Alobi, M.M. Sambo, Adsorption and quantum chemical studies on the inhibition of the corrosion of aluminium in HCl by *Gloriosa superba* (Gs) gum, Chem. Eng. Commun. 201 (2014) 1360-1383.
[12] N.O. Eddy, H. Momoh-Yahaya, E.E. Oguzie, Theoretical and experimental studies on the corrosion inhibition potentials of some purines for aluminum in 0.1 M HCl, J. Adv. Res. 6 (2015) 203-216.
[13] L.M. Vracarand, D.M. Drazic, Adsorption and corrosion inhibitive properties of some organic molecules on iron electrode in sulfuric acid, Corr. Sci. 44 (2002) 1669-1681.
[14] I. Danaee, N.N. Khomami, A.A. Attar, Corrosion of AISI 4130 steel alloy under hydrodynamic condition in ethylene glycol + water + NO_2^- Solution, J. Mater. Chem. Phy. 29 (2010) 89-96.
[15] P.C. Okafor, Y. Zheng, Synergistic inhibition behaviour of methylbenzyl quaternary imidazoline derivative and iodided ions on mild steel in H_2SO_4solutions, Corros. Sci. 51 (2009) 850-859.
[16] P.O. Ameh, P. Ukoha, N.O. Eddy, Experimental and quantum chemical studies on the corrosion inhibition potential of phthalic acid for mild steel in 0.1 M H_2SO_4, Chem. Sci. J. 6 (2015) 1-8
[17] K.S. Jacob, G. Parameswaran, Corrosion inhibition of mild steel in hydrochloric acid solution by Schiff base furointhiosemicarbazone, Corros. Sci. 52 (2010) 224-228.
[18] S.S. Abd El-Rehim, H.H. Hassan, M.A. Amin, Corrosion inhibition study of pure Al and some of its alloys in 1.0 M HCl solution by impedance technique, Corros. Sci. 46 (2004) 5-25.
[19] M. Benabdellah, R. Touzani, A. Aouniti, A. Dafali, S. El-Kadiri, B. Hammouti, Inhibitive action of some bipyrazolic compounds on the corrosion of steel in 1 M HCl Part I: Electrochemical study, J. Mater. Chem. Phy. 105 (2007) 373-379.
[20] K.F. Khaled, M.M. Al-Qahtani, The inhibitive effect of some tetrazole derivatives towards Al corrosion in acid solution: Chemical, electrochemical and theoretical studies, Mater. Chem. Phy. 113 (2009) 150-158.
[21] M. Jeeva, G.V. Prabhu, M.S. Boobalan, C.M. Rajesh, Interactions and inhibition effect of urea-derived mannich bases on a mild steel surface in HCl, J. Phys. Chem. 119 (2015) 22025-22043.
[22] R.S. Abdel Hameed, Ranitidine drugs as non-toxic corrosion inhibitors for mild steel in hydrochloric acid medium, Portug. Electrochim. Acta 29 (2011) 273-285.
[23] P. Lowmunkhong, D. Ungthararak, P. Sutthivaiyakit, Tryptamine as a corrosion inhibitor of mild steel in hydrochloric acid solution, Corros. Sci. 52 (2010) 30-36.
[24] D. Gopi, M.S. El-Sayed, Manivannan, D. Rajeswari, M. Surendiran, L. Kavitha, Corrosion and corrosion inhibition of mild steel in groundwater at different temperatures by newly synthesized benzotriazole and phosphorus derivatives, Indust. Eng. Chem. Res. 53 (2014) 4286-4294.
[25] G. Gao, C. Liang, Electrochemical and DFT studies of beta-aminoalcohols as corrosion inhibitors for brass, Electrochim. Acta 52 (2007) 4554-4559.
[26] N.O. Eddy, Theoretical study on some amino acids and their potential activity as corrosion inhibitors for mild steel in HCl, Mol. Simul. 35 (2010) 354-363.
[27] N.O. Eddy, E.E. Ebenso, Quantum chemical studies on the inhibition potentials of some penicillin compounds for the corrosion of mild steel in 0.1 M HCl, J. Mol. Mod. 16 (2010) 1291-1306.
[28] N.O. Eddy, B.I. Ita, QSAR, DFT and quantum chemical studies on the inhibition potentials of some carbozones for the corrosion of mild steel in HCl, J. Mol. Mod. 17 (2010) 359-376.
[29] H. Ju, Z.P. Kai, Y. Li, Aminic nitrogen-bearing polydentate Schiff base compounds as corrosion inhibitors for iron in acidic media: a quantum chemical calculation, Corros. Sci. 50 (2008) 865-871.
[30] A.Y. Musa, R.T. Jalgham, A.B. Mohamad, Molecular dynamic and quantum chemical calculations for phthalazine derivatives as corrosion inhibitors of mild steel in 1 M HCl, Corros. Sci. 56 (2012) 176-183.
[31] F. Bentiss, M. Bouanis, B. Mernari, M. Traisnel, H. Vezin, M. Lagrenee, Understanding the adsorption of 4H-1,2,4triazole derivatives on mild steel surface in molar hydrochloric acid, Appl. Surf. Sci. 253 (2007) 3696-3704.
[32] B. Gomez, N.V. Likhanova, M.A. Sominguez-Aguiliar, R. Martinez-Palou, A. Vela, L. Gazquez, Quantum chemical study of the inhibitive properties of 2-pyridyl-Azoles, J. Phys. Chem. B 110 (2006) 8928-8934.

Cite this Article as: P.O. Ameh, P. Ukoha, P. Ejikeme, N.O. Eddy, Experimental and computational chemistry studies on the inhibition of the corrosion of mild steel in 0.1 M H_2SO_4 by 4-hydroxylbenzoic acid, J. Adv. Electrochem. 2(1) (2016) 60–66.